Detection of Polycyclic Aromatic Hydrocarbons in High Organic Carbon Ultrafine Particle Extracts by Electrospray Ionization Ultrahigh-Resolution Mass Spectrometry

Eric Schneider, Barbara Giocastro, Christopher P. Rüger,* Thomas W. Adam, and Ralf Zimmermann

Cite This: *J. Am. Soc. Mass Spectrom.* 2022, 33, 2019–2023 | Read Online

ACCESS | Metrics & More | Article Recommendations | SI Supporting Information

ABSTRACT: The detection of polycyclic aromatic hydrocarbons (PAHs) by electrospray ionization (ESI) without additional reagents or targeted setup changes to the ionization source was observed in ultrafine particle (UFP) extracts, with high organic carbon (OC) concentrations, generated by a combustion aerosol standard (CAST) soot generator. Particulate matter (PM) was collected on filters, extracted with methanol, and analyzed by ESI Fourier-transform ion cyclotron resonance mass spectrometry (FT-ICR MS). Next to oxygen-containing species, pure hydrocarbons were found to be one of the most abundant compound classes, detected as $[M + Na]^+$ or $[M + H]^+$ in ESI+ and mostly as $[M - H]^-$ in ESI−. The assigned hydrocarbon elemental compositions are identified as PAHs due to their high aromaticity index (AI > 0.67) and were additionally confirmed by MS/MS experiments as well as laser desorption ionization (LDI). Thus, despite the relatively low polarity, PAHs have to be considered in the molecular attribution of these model aerosols and/or fresh emissions with low salt content investigated by ESI.
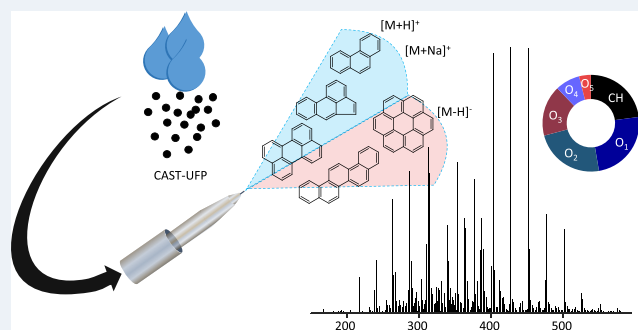
INTRODUCTION

Polycyclic aromatic hydrocarbons (PAHs) are frequently emitted by incomplete combustion processes of most carbonaceous fuel types, e.g., fossil fuel, biomass, and are therefore frequently found as pollutants in the environment. Additionally, PAHs induce strong toxicological effects, including carcinogenic effects through reactive metabolites, which are also a source of reactive oxygen species (ROS), which induce oxidative stress.[1,2] Therefore, when analyzing the chemical composition of particulate matter (PM), the identification of PAHs is of high interest. Anthropogenic emission of particulate matter from industrial or urban sources like engines or biomass burning, is responsible for global adverse health effects.[3] Ultrafine particles (UFP, aerodynamic diameter ≤100 nm) are of particular interest due to their high particle number concentrations, as well as high capability to adsorb toxic compounds to their surface and the ability to transport these compounds deep into the respiratory system.[1,4]

Electrospray ionization (ESI) is a frequently applied ionization technique for the analysis of liquid aerosol extracts, due to its softness and sensitive ionization of polar compounds (e.g., oxygen-containing functionalities), which are frequently found in aerosol samples.[5,6] Nonpolar compounds like PAHs are usually not observed under standard ESI conditions, due to their poor ionization efficiency and ionization suppression from more readily ionized polar molecules.[7] For nonpolar compounds, atmospheric pressure photoionization (APPI) or

laser desorption ionization (UV-LDI) have recently been established as comprehensive ionization techniques, but with the drawback of a lower sensitivity for highly oxygenated compounds.[8]

The unexpected detection of PAHs in addition to a range of oxygenated species under standard ESI conditions of a model PM extract is reported here, representing fresh high organic carbon (OC) soot emissions as well as similar artificially generated aerosols. With detectability of PAHs within the fresh low-polar PM, misattribution and missing their contribution, also in ESI spectra, will be addressed in this short communication.
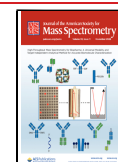
EXPERIMENTAL SECTION

Sample Preparation. A combustion aerosol standard (CAST) soot generator operated with propane was used to generate high organic carbon ultrafine particles. PM was collected on quartz fiber filters (47 mm diameter), and one-half of each filter was placed in a prebaked extraction vial and

then extracted with 5 mL of methanol (LC-MS grade) under shaking for 30 min. The extracts were filtered through a 0.2 μm PTFE membrane (Sartorius, Goettingen, Germany) in a stainless-steel filter holder via a glass syringe and stored at $-25\,°C$ until further analysis.

ESI/LDI-FTICR-MS Measurements. Ultrahigh-resolution FT-ICR-MS measurements were carried out on a SolariX (Bruker Daltonik, Bremen, Germany) equipped with a 7 T superconducting magnet. The samples were analyzed in positive and negative ionization mode with a direct-infusion ESI ion source setup (Bruker Daltonik, API Ion Source). The following ionization parameter were selected for positive/negative ion mode (ESI $\pm$) respectively: capillary voltage $-3.3/3.7$ kV, drying gas temperature 180 °C, drying gas flow rate 4.0 L/min, nebulizer gas flow rate 1.4 bar, quadrupole mass m/z 120, and syringe flow rate 300 μL/h. 200/300 scans were collected for each measurement with a 1.96 s (4M) transient and a resulting resolving power of >310000 at m/z 400.

For laser desorption/ionization (UV-LDI) experiments, 20 μL of the respective extracts was spiked on multiple spots of the LDI-target-plate, and the solvent was allowed to evaporate. The number of laser shots was set to 100, with a laser frequency of 500 Hz and a laser power of 25%.

Data Analysis. Raw data were peak picked (cutoff: S/N = 9) and exported with Bruker Data Analysis 5.1 (Bruker Daltonik, Bremen, Germany). The exported mass spectra were processed by self-written MATLAB algorithms and routines combined in a graphical user interface named CERES Processing. After careful investigation and consideration of reasonable attribution boundaries, we deployed the following restrictions for elemental composition assignment in the range of 120−1000 Da with an assignment error of <1 ppm: $C_cH_hO_oNa_{na}$; $6 \leq c \leq 100$, $6 \leq h \leq 200$, $o \leq 5$, $na \leq 1$. Additional restrictions were applied for the H/C ratio: 0.4−2.4, O/C ratio: 0−1.4, and double bond equivalents: DBE 0−50. DBE and aromaticity index (AI) calculations are described in the Supporting Information.[9] Blank filters were processed according to the same procedure and used for blank correction. For ESI measurements, data from triplicate filter samples generated from the repetition of the same experimental CAST conditions were combined for data evaluation, including only sum formulas found in at least two measurements.

■ RESULTS AND DISCUSSION

Both ESI polarities display a high molecular complexity of elemental compositions within the CHO_x (x = 0−5) compound class (Figures 1 and S1), mainly in the range of m/z 150−800 (ESI+, 900 formulas) or m/z 150−600 (ESI-, 500 formulas). Oxygenated species are the dominant group in both polarities, as would be expected for ionization with ESI, which is sensitive to polar compounds (i.e., oxygen-containing functional groups).[5] While in ESI− mostly [M − H]$^-$ ions are observed (some [M]$^{•-}$), in ESI+ [M + Na]$^+$ adduct-ions are most common, with only minor contributions of [M + H]$^+$ ions.

Remarkably, it was also possible to detect high numbers of signals containing only CH (ESI $\pm$: 180/120 sum formulas, counting Na$^+$ and H$^+$ adducts each). The CH formulas contain an average of 32/29 carbon atoms and show exclusively particularly high DBE values in a narrow range ($\overline{DBE}_{ESI+}$= 22 $\pm$ 11, $\overline{DBE}_{ESI-}$= 21 $\pm$ 8, Figure S2), as well as high aromaticity
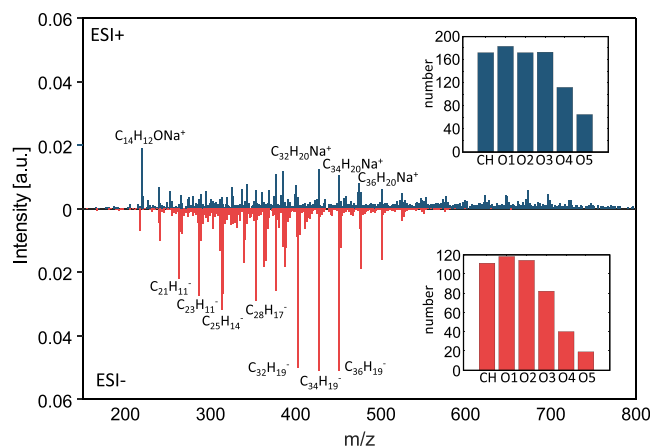

Figure 1. ESI-FTICR-MS mass spectra of intensities normalized to the total sum of intensity with ESI+ data in blue (top) and ESI− data in red (bottom). Prominent peaks are labeled with their assigned elemental composition. Compound class formula number distribution of ESI$\pm$ as insets (right).

indices of 0.66/0.74 in ESI$\pm$, which suggests the classification as condensed polycyclic aromatic hydrocarbons (PAHs) from a pyrogenic process. This is stressed by the distribution displayed in Figure 2, which shows predominantly AI values
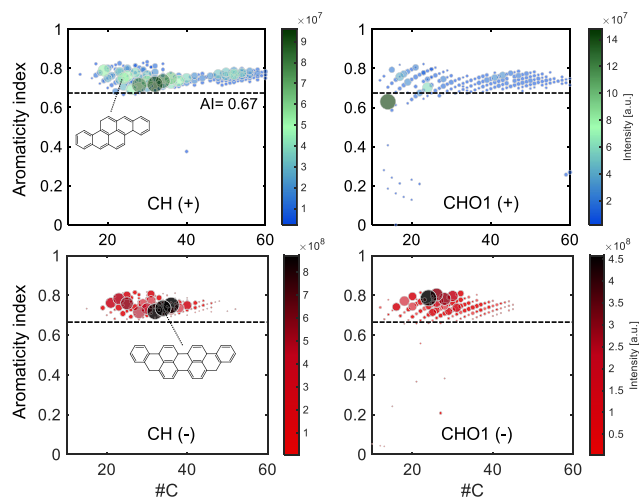

Figure 2. Aromaticity index versus carbon number (#C) plot of CH and CHO_1 compound classes in ESI$\pm$ with exemplary molecular structures. AI > 0.67 indicated by a dotted line to highlight region of condensed aromatic molecules.

larger than the frequently applied limit for condensed aromatic structures of AI > 0.67.[9] Oxygen-containing molecules observed here show similar properties regarding their aromaticity. This leads to the conclusion that these species are formed through the partial oxidation of aromatic core molecules, which are precursors in soot formation,[10] during the propane combustion process in the CAST or shortly afterward in the still-hot exhaust area. Consequently, this model aerosol serves as an example for other artificially generated PM or fresh soot emissions, e.g., from coal combustion or malfunctioning engines.

As ESI is sensitive for the detection of even low concentrations of polar compounds, it is possible to detect

these CHO_{1-5} species that are not accessible by, e.g., gas chromatography. In most cases, CH species are not ionized by direct-infusion ESI due to their poor ionization efficiency based on the lack of polar moieties and consequently strong matrix effects/ion suppression.[11] To overcome this limitation, derivatization with tropylium ions or cationization with Ag(I) can be applied to improve the detection of PAHs, e.g., in LC-ESI-MS, through the formation of adduct ions which are subsequently fragmented by collision induced dissociation (CID) to generate radical molecule cations.[12−15] Another way of generating radical cations is the application of chemical electron transfer reagents (e.g., oxidants) like trifluoroacetic acid (TFA) or SbF_5.[16]

Other reports of PAH ionization by ESI, e.g., from heavy crude oil asphaltenes,[17] Arabian mix vacuum residue,[7,18] coal fire sponge extracts,[19] or individual PAHs,[11,20] describe the formation of protonated molecule-ions by addition of acid to the solvents or the formation of radical cations by abstraction of an electron at the surface of the ESI spray capillary,[21] but no dominant PAH-sodium-adduct formation.

Additionally, to the best of our knowledge, the detection of PAHs by ESI− has not been reported, particularly not for this PM matrix. In the case of this ultrafine particle model aerosol with a high share of organic carbon (OC, 0.02 mg C/m^3), PAHs are found to be the main fraction of OC with concentrations of 3−6 ring PAHs in the range of 10−700 ng/m^3 (PM) and 1−20 ppb (extract, EPA PAH, Table S1). The high concentrations of PAHs in combination with low concentrations of polar compounds, that would compete for charges during the ionization process of ESI and therefore suppress the ionization of PAH, seem to enable the ionization of CH species as adduct ions in ESI+.

The observation of CH species with ESI from the methanol filter extracts was also confirmed by LDI-FTICR-MS measurements, (Figure S3) that identified at least 35 CH compounds matching the ESI data. UV-LDI is a selective method for the detection of PAHs up to high m/z due to their suitable light-absorbing properties.[8] Additionally, ESI-FTICR-MS/MS experiments of selected peaks by CID provide supporting structural information (Figures 3 and S4). For example, the MS/MS spectrum of $C_{24}H_{12}Na$ (measured m/z: 323.08304) shows only three fragment signals, which match possible fragment-sodium adducts of condensed polycyclic aromatic

ring structures comparable to coronene and its structural isomers. As expected from condensed aromatic ring structures, the relative intensity of fragments is low. Furthermore, when increasing the CID energy, the intensity of the fragment ions is not increased (Figure S5). At a higher CID energy, the charge carrying sodium is abstracted from the molecule, before more pronounced fragmentation of C−C bonds occurs. Therefore, the detection of elemental compositions by both ionization techniques creates high certainty for the assignment of CH compounds in ESI as PAHs. When comparing ESI data from positive and negative ionization mode, it is apparent that ESI+ is better suited for the ionization of PAHs, as more compounds are detected, especially for $m/z > 500$. Still, there is a significant overlap of compounds found in both ionization modes matching multiring pyrogenic soot precursors (Figure S6), e.g. $C_{32}H_{20}$, $C_{34}H_{20}$, $C_{36}H_{20}$.

Aromatic structures can stabilize a negative charge in molecules after deprotonation as the number of π-electrons, forming the delocalized aromatic π-system.[22] For planar aromatic CH compounds without electron-donating non-aromatic C−H bonds, which may be deprotonated due to higher acidity, $[M]^{\bullet-}$ are also observed. As PAHs have a comparably high electron affinity, they can stabilize an electron by electron attachment, as was previously discussed for negative LDI of a PAH rich asphaltene fraction.[23]

In ESI+, mostly sodium adducts of PAHs are observed. This behavior could be explained by the ability of polycyclic aromatic ring systems to form adduct bonds with sodium ions (cation-π interaction), that are relatively stable and consequently able to withstand the ion transfer plus even some CID voltage (Figure S5).[24,25] The sodium-π interaction of PAHs in ESI may be a point of future work, to increase the understanding of this effect, especially regarding the relevance of PAHs in environmental samples, such as aerosols.

CONCLUSION

In summary, polycyclic aromatic hydrocarbons were detected up to m/z 800 by ionization with ESI in negative and positive ionization modes, in polar extracts of high organic carbon ultrafine particles generated by a CAST. PAHs in ESI+ were mainly detected as sodium adducts, while predominately deprotonation was observed in ESI−. The identification of PAHs was also confirmed by LDI and ESI-MS/MS experiments. High concentrations of PAHs from the artificial, but not unrealistic, aerosol sample enable the ionization of nonpolar PAHs without any derivatization or acidification, although polar species (CHO_x) are also abundant. Future experiments investigating similar, high organic carbon aerosols need to be open for the possibility of the detection of nonpolar CH compounds with ESI in both ionization modes to avoid errors in formula assignments and data interpretation.

ASSOCIATED CONTENT

Ⓢ Supporting Information

The Supporting Information is available free of charge at https://pubs.acs.org/doi/10.1021/jasms.2c00163.

Additional mass spectrometric data and GC-MS results (PDF)

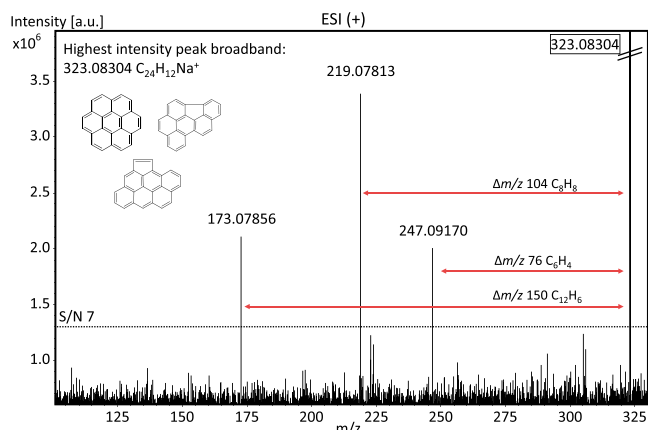**Figure 3.** CID-MS/MS-FTICR spectrum of nominal mass m/z 323 in ESI+ (CID = 5 V). Elemental composition assigned to molecular ion $C_{24}H_{12}Na^+$ with potential isomeric structures displayed.

■ AUTHOR INFORMATION

Corresponding Author

Christopher P. Rüger − *Joint Mass Spectrometry Centre (JMSC), Chair of Analytical Chemistry, University Rostock, 18059 Rostock, Germany; Department Life, Light & Matter (LLM), University of Rostock, 18059 Rostock, Germany;* orcid.org/0000-0001-9634-9239; Email: christopher.rueger@uni-rostock.de

Authors

Eric Schneider − *Joint Mass Spectrometry Centre (JMSC), Chair of Analytical Chemistry, University Rostock, 18059 Rostock, Germany; Department Life, Light & Matter (LLM), University of Rostock, 18059 Rostock, Germany*

Barbara Giocastro − *Institute of Chemistry and Environmental Engineering, University of the Bundeswehr Munich, 85579 Neubiberg, Germany*

Thomas W. Adam − *Institute of Chemistry and Environmental Engineering, University of the Bundeswehr Munich, 85579 Neubiberg, Germany; Joint Mass Spectrometry Center (JMSC) at Comprehensive Molecular Analytics (CMA), Helmholtz Munich, 85764 Neuherberg, Germany*

Ralf Zimmermann − *Joint Mass Spectrometry Centre (JMSC), Chair of Analytical Chemistry, University Rostock, 18059 Rostock, Germany; Department Life, Light & Matter (LLM), University of Rostock, 18059 Rostock, Germany; Joint Mass Spectrometry Center (JMSC) at Comprehensive Molecular Analytics (CMA), Helmholtz Munich, 85764 Neuherberg, Germany*

Complete contact information is available at:
https://pubs.acs.org/10.1021/jasms.2c00163

Notes

The authors declare no competing financial interest.

■ REFERENCES

(1) Li, N.; Georas, S.; Alexis, N.; Fritz, P.; Xia, T.; Williams, M. A.; Horner, E.; Nel, A. A work group report on ultrafine particles (American Academy of Allergy, Asthma & Immunology): Why ambient ultrafine and engineered nanoparticles should receive special attention for possible adverse health outcomes in human subjects. *Journal of allergy and clinical immunology* **2016**, *138* (2), 386−396.

(2) Stading, R.; Gastelum, G.; Chu, C.; Jiang, W.; Moorthy, B. Molecular mechanisms of pulmonary carcinogenesis by polycyclic aromatic hydrocarbons (PAHs): Implications for human lung cancer. *Seminars in cancer biology* **2021**, *76*, 3−16.

(3) Di, Q.; Wang, Y.; Zanobetti, A.; Wang, Y.; Koutrakis, P.; Choirat, C.; Dominici, F.; Schwartz, J. D. Air Pollution and Mortality in the Medicare Population. *New England journal of medicine* **2017**, *376* (26), 2513−2522.

(4) Juarez Facio, A. T.; Yon, J.; Corbière, C.; Rogez-Florent, T.; Castilla, C.; Lavanant, H.; Mignot, M.; Devouge-Boyer, C.; Logie, C.; Chevalier, L.; Vaugeois, J.-M.; Monteil, C. Toxicological impact of organic ultrafine particles (UFPs) in human bronchial epithelial BEAS-2B cells at air-liquid interface. *Toxicology in vitro* **2022**, *78*, 105258.

(5) Song, J.; Li, M.; Fan, X.; Zou, C.; Zhu, M.; Jiang, B.; Yu, Z.; Jia, W.; Liao, Y.; Peng, P. Molecular Characterization of Water- and Methanol-Soluble Organic Compounds Emitted from Residential Coal Combustion Using Ultrahigh-Resolution Electrospray Ionization Fourier Transform Ion Cyclotron Resonance Mass Spectrometry. *Environ. Sci. Technol.* **2019**, *53* (23), 13607−13617.

(6) Schneider, E.; Czech, H.; Popovicheva, O.; Lütdke, H.; Schnelle-Kreis, J.; Khodzher, T.; Rüger, C. P.; Zimmermann, R. Molecular Characterization of Water-Soluble Aerosol Particle Extracts by Ultrahigh-Resolution Mass Spectrometry: Observation of Industrial Emissions and an Atmospherically Aged Wildfire Plume at Lake Baikal. *ACS Earth Space Chem.* **2022**, *6* (4), 1095−1107.

(7) Miyabayashi, K.; Naito, Y.; Tsujimoto, K.; Miyake, M. Structure characterization of polyaromatic hydrocarbons in Arabian mix vacuum residue by electrospray ionization Fourier transform ion cyclotron resonance mass spectrometry. *Int. J. Mass Spectrom.* **2004**, *235* (1), 49−57.

(8) Apicella, B.; Carpentieri, A.; Alfè, M.; Barbella, R.; Tregrossi, A.; Pucci, P.; Ciajolo, A. Mass spectrometric analysis of large PAH in a fuel-rich ethylene flame. *Proc. Combust. Inst.* **2007**, *31* (1), 547−553.

(9) Koch, B. P.; Dittmar, T. From mass to structure: an aromaticity index for high-resolution mass data of natural organic matter. *Rapid Commun. Mass Spectrom.* **2006**, *20* (5), 926−932.

(10) Haynes, B. S.; Wagner, H. Soot formation. *Prog. Energy Combust. Sci.* **1981**, *7* (4), 229−273.

(11) Hettiyadura, A. P. S.; Laskin, A. Quantitative analysis of polycyclic aromatic hydrocarbons using high-performance liquid chromatography-photodiode array-high-resolution mass spectrometric detection platform coupled to electrospray and atmospheric pressure photoionization sources. *J Mass Spectrom .* **2021**, *57* (2), e4804.

(12) Takino, M.; Daishima, S.; Yamaguchi, K.; Nakahara, T. Determination of polycyclic aromatic hydrocarbons by liquid chromatography—electrospray ionization mass spectrometry using silver nitrate as a post-column reagent. *J. Chromatogr. A* **2001**, *928* (1), 53−61.

(13) Lien, G.-W.; Chen, C.-Y.; Wu, C.-F. Analysis of polycyclic aromatic hydrocarbons by liquid chromatography/tandem mass spectrometry using atmospheric pressure chemical ionization or electrospray ionization with tropylium post-column derivatization. *Rapid Commun. Mass Spectrom.* **2007**, *21* (22), 3694−3700.

(14) Ghislain, T.; Faure, P.; Michels, R. Detection and monitoring of PAH and oxy-PAHs by high resolution mass spectrometry: comparison of ESI, APCI and APPI source detection. *J. Am. Soc. Mass Spectrom.* **2012**, *23* (3), 530−536.

(15) Maziarz, E. P., III; Baker, G. A.; Wood, T. D. Electrospray ionization Fourier transform mass spectrometry of polycyclic aromatic hydrocarbons using silver(I)-mediated ionization. *Can. J. Chem.* **2005**, *83* (11), 1871−1877.

(16) van Berkel, G. J.; Asano, K. G. Chemical Derivatization for Electrospray Ionization Mass Spectrometry. 2. Aromatic and Highly Conjugated Molecules. *Anal. Chem.* **1994**, *66* (13), 2096−2102.

(17) Molnárné Guricza, L.; Schrader, W. Electrospray ionization for determination of non-polar polyaromatic hydrocarbons and poly-aromatic heterocycles in heavy crude oil asphaltenes. *J Mass Spectrom .* **2015**, *50* (3), 549−557.

(18) Miyabayashi, K.; Suzuki, K.; Teranishi, T.; Naito, Y.; Tsujimoto, K.; Miyake, M. Molecular Formula Determination of Constituents in Arabian Mix Vacuum Residue by Electrospray Ionization Fourier Transform Ion Cyclotron Resonance Mass Spectrometry. *Chem. Lett.* **2000**, *29* (2), 172−173.

(19) Xu, D.; Liang, Y.; Hong, X.; Liang, M.; Liang, H. Specification of complex-PAHs in coal fire sponges (CFS) by high-resolution mass spectrometry with electrospray ionization. *Environ. Sci. Pollut. Res.* **2021**, DOI: 10.1007/s11356-021-12929-3.

(20) Cha, E.; Jeong, E. S.; Han, S. B.; Cha, S.; Son, J.; Kim, S.; Oh, H. B.; Lee, J. Ionization of Gas-Phase Polycyclic Aromatic Hydrocarbons in Electrospray Ionization Coupled with Gas Chromatography. *Analytical chemistry* **2018**, *90* (6), 4203−4211.

(21) van Berkel, G. J.; McLuckey, S. A.; Glish, G. L. Electrochemical origin of radical cations observed in electrospray ionization mass spectra. *Anal. Chem.* **1992**, *64* (14), 1586−1593.

(22) Hückel, E. Quantentheoretische Beiträge zum Benzolproblem. *Eur. Phys. J. A Hadron. Nucl.* **1931**, *70* (3−4), 204−286.

(23) Pereira, T. M.C.; Vanini, G.; Tose, L. V.; Cardoso, F. M.R.; Fleming, F. P.; Rosa, P. T.V.; Thompson, C. J.; Castro, E. V.R.; Vaz, B. G.; Romao, W. FT-ICR MS analysis of asphaltenes: Asphaltenes go in, fullerenes come out. *Fuel (Lond)* **2014**, *131*, 49−58.

(24) Yourdkhani, S.; Chojecki, M.; Korona, T. Substituent effects in the so-called cation𝜋 interaction of benzene and its boron-nitrogen doped analogues: overlooked role of σ-skeleton. *Phys. Chem. Chem. Phys.* **2019**, *21* (12), 6453−6466.

(25) Ma, J. C.; Dougherty, D. A. The Cation-π Interaction. *Chem. Rev.* **1997**, *97* (5), 1303−1324.

📖 Recommended by ACS

Heat Pulse Desorption of Low-Volatility Compounds by a Heated N₂ Gas Pulse with Mass Spectrometry

Satoshi Ninomiya, Kenzo Hiraoka, *et al.*
OCTOBER 13, 2022
JOURNAL OF THE AMERICAN SOCIETY FOR MASS SPECTROMETRY READ

Chemical Characterization and Quantitation of Phenols in Fuel Extracts by Using Gas Chromatography/Methane Chemical Ionization Triple Quadrupole Mass Spectrometry

Jacob D. Guthrie, Hilkka I. Kenttämaa, *et al.*
SEPTEMBER 26, 2022
ENERGY & FUELS READ

Profiling Olefins in Gasoline by Bromination Using GC×GC-TOFMS Followed by Discovery-Based Comparative Analysis

Timothy J. Trinklein, Robert E. Synovec, *et al.*
JUNE 21, 2022
ANALYTICAL CHEMISTRY READ

Focusing on Volatile Organic Compounds of Natural Resins by Selected-Ion Flow Tube-Mass Spectrometry

Camilla Guerrini, Erika Ribechini, *et al.*
JUNE 28, 2022
JOURNAL OF THE AMERICAN SOCIETY FOR MASS SPECTROMETRY READ

Get More Suggestions >